INTERNATIONAL JOURNAL FOR NUMERICAL METHODS IN FLUIDS
Int. J. Numer. Meth. Fluids 2008; **56**:1597–1603
Published online 2 October 2007 in Wiley InterScience (www.interscience.wiley.com). DOI: 10.1002/fld.1594

Turbulent mixing in spherical implosions

David L. Youngs*,† and Robin J. R. Williams

AWE Aldermaston RG7 4PR, U.K.

SUMMARY

We discuss the application of the numerical code TURMOIL to turbulent mixing in a simple spherical implosion, a much simplified version of an inertial confinement fusion implosion. Some form of Monotone integrated large eddy simulation is required to eliminate non-physical oscillations, as shocks and contact discontinuities are present. The dissipation in the TURMOIL scheme is analysed. It is argued that this is relatively low and that the 'sub-grid' dissipation can be precisely quantified. © British Crown Copyright 2007/MOD. Reproduced with permission. Published by John Wiley & Sons, Ltd.

Received 25 April 2007; Revised 13 July 2007; Accepted 13 July 2007

KEY WORDS: large eddy simulation; compressible flow

1. INTRODUCTION

A large eddy simulation (LES) technique, TURMOIL, which uses a Lagrange-remap finite difference numerical method, has been very successfully applied to a range of Rayleigh-Taylor (RT) and Richtmyer-Meshkov (RM) mixing problems [1, 2]. In the Lagrange phase, artificial viscosity models dissipation due to shocks. The remap phase uses third-order monotonic advection; the resulting implicit dissipation provides the 'sub-grid' dissipation required for turbulence simulations. Here, we analyse the dissipation in this scheme. It is argued that this is relatively low and that the sub-grid dissipation can be precisely quantified. It is shown that TURMOIL performs very well at low Mach numbers. For Godunov schemes, at least those widely used at present, dissipation can become large as the Mach number becomes small [3]. To illustrate this point, TURMOIL results

*Correspondence to: David L. Youngs, AWE Aldermaston RG7 4PR, U.K.
†E-mail: david.youngs@awe.co.uk

are compared with those from a piecewise parabolic method (PPM) method for a simple Kelvin–Helmholtz test problem. Low Mach number behaviour is very important in compressible LES as, even in highly compressible flow, the Mach number of the turbulence is usually low.

Results are also shown for a simple spherical implosion, a much simplified version of an inertial confinement fusion (ICF) implosion. The two fluids are miscible and viscosities are assumed to be very small so that high Reynolds number turbulent mixing occurs. A spherical polar mesh is used to calculate the mixing. During the implosion both RT and RM instabilities occur. The effect of mesh size is investigated and it is concluded that the averaged properties of the mixing zone are close to being mesh converged.

2. A SIMPLE SPHERICAL IMPLOSION

The initial geometry for the unperturbed spherical implosion, in dimensionless units, has density $\rho = 0.05$ for $0 \leqslant r < 10$ and $\rho = 1.0$ for $10 \leqslant r < 12$, with pressure $p = 0.1$ throughout. Perfect gas equations of state are used with $p = (\gamma - 1)e$, where e is the specific internal energy and $\gamma = \frac{5}{3}$. The ratio of the specific heats between the two fluids is 20:1, giving equal initial temperatures in the two regions. The implosion is driven by applying a varying pressure at the outer boundary, which moves with the flow from $r = 12$ initially. The applied pressure is $p = 10.0$ for $0 < t < 0.5$, thereafter decreasing linearly to $p = 0.0$ at $t = 3.0$.

The radius–time plot obtained from a 1D Lagrangian calculation is shown in Figure 1. RM instability occurs when the incident shock wave passes through the interface between fluids at $t \sim 0.5$, amplifying the initial perturbation. Turbulent mixing occurs towards the end of the implosion, when the interface decelerates, due to a combination of RT and RM instabilities.

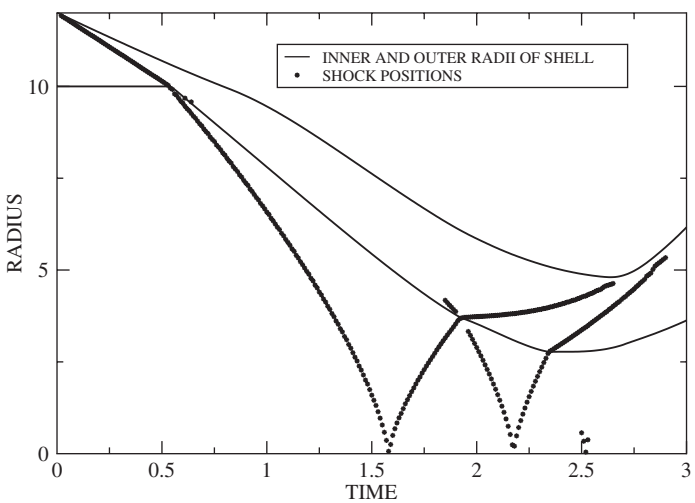

Figure 1. Radius–time plot for the spherical implosion. Solid lines: boundaries of the dense spherical shell. Stars: shock positions.

DOI: 10.1002/fld

3. THE NUMERICAL METHOD

3.1. The Lagrange-remap method

TURMOIL uses a Lagrange-remap method [4]. A mass fraction advection equation is used for gas mixtures [2]. The Lagrange phase calculates the changes in velocity and internal energy due to the pressure field. A staggered mesh is used with velocity components defined at cell corners and with density, mass fraction and internal energy defined at cell centres. A finite difference approximation is used which is second-order accurate in space and time and conserves total energy. Quadratic artificial viscosity, q, is used to provide the dissipation due to shocks, where $q \sim \rho \Delta x^2 (\partial u/\partial x)^2$ for 1D problems. In this section, partial derivatives denote centred differences. There are oscillations behind shocks—the treatment of shocks is not as good as in second-order Godunov methods. However, the method does have one very useful property: the irreversible dissipation of kinetic energy in the Lagrangian phase,

$$\varepsilon_{\mathrm{L}} = -q \nabla \cdot \mathbf{u} \tag{1}$$

is negligible for low Mach number, near incompressible flow. All three spatial directions are calculated simultaneously in the Lagrange phase.

The remap phase calculates advective fluxes and may be regarded as a mapping of the configuration at the end of the Lagrangian phase back to the original mesh. Alternatively, near-Lagrangian mesh motion can be used in the radial direction to reduce numerical diffusion in implosion problems. The advection is calculated in separate 1D sweeps using a third-order monotonic method based on the work of van Leer. The order of the sweeps is reversed every time step. Several Lagrange steps may be performed per remap step, significantly increasing the efficiency of low Mach number calculations. The method gives exact monotonic behaviour i.e. fluid variables at the end of the remap phase lie with the range of neighbouring values at the end of the Lagrange phase.

The remap phase conserves mass, internal energy and momentum. However, kinetic energy is dissipated. The loss of kinetic energy in the remap phase, ε_{R}, may be quantified precisely as a function of position by the simple algebraic technique of DeBar [5] and may be added on to the internal energy to recover total energy conservation. This technique may also be used to quantify the 'sub-grid' dissipation. For small time steps the algebraic DeBar formula can be interpreted as a numerical approximation to the differential form:

$$\varepsilon_{\mathrm{R}} \simeq \sum_{i,j} \frac{1}{2} \rho |u_i| \Delta_j u_i \frac{\partial u_i}{\partial x_j} \tag{2}$$

where $\Delta_j u_i$ is the velocity jump for u_i in the x_j direction constructed at the momentum cell boundary for calculation of the monotonic advection flux. Dissipation occurs where there are steep velocity gradients and is negligible in well-resolved flow regions, where $\Delta u \to 0$. The resulting dissipation is comparable with that obtained with an explicit sub-grid-scale model.

3.2. Low Mach number behaviour

The spherical implosion is driven by strong shocks. However, the turbulence Mach number is relatively low (~ 0.1) and at the end of the implosion, when most of the mixing occurs, the flow

DOI: 10.1002/fld

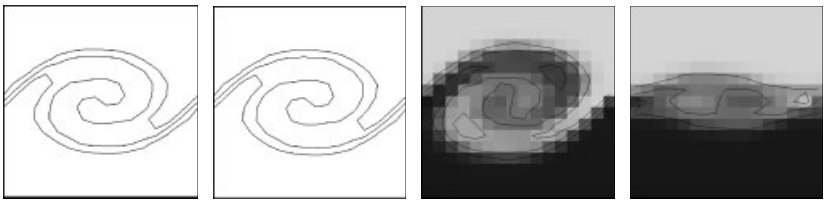

Figure 2. Low Mach number behaviour for Kelvin–Helmholtz test problem.
Left: TURMOIL. Right: PPM calculation.

is weakly compressible between shocks. Hence, it is essential that the numerical method used has an adequate treatment for shocks and good behaviour at low Mach number. The latter can be characterized by a simple example, the roll-up of a vortex sheet. Figure 2 shows TURMOIL results using 16×16 zones at Mach numbers (initial velocity difference/sound speed) of 0.2 and 0.02. The results are almost identical, as expected in this limit.

It is interesting to consider what would happen if a second-order Godunov method were used in the Lagrange phase. This could certainly give a better treatment for shocks. Figure 2 includes results obtained with VH1, a freely available Godunov code, which uses a PPM Lagrange-remap method [6]. With this code, the vortex is strongly dissipated at $M = 0.02$. It was shown in [3] that the dissipation in first-order Godunov methods increases as the Mach number is reduced. Now it is apparent from Equation (2) that the scheme must generate non-zero velocity jumps where there is unresolved structure in order to provide the required sub-grid dissipation. The test problem (chosen to represent a poorly resolved eddy in a LES) suggests that the dissipation at small scales is significantly enhanced in strictly monotone Godunov schemes.

Further insight comes from RM Christensen, see Benson [7], who argued that the use of a Godunov method in a 1D Lagrangian calculation is approximately equivalent to using a 'monotonic q'

$$q^{\text{mono}} = -\left(\frac{1}{2}\rho c \Delta u + \frac{\gamma+1}{2}\rho|\Delta u|\Delta u\right) \tag{3}$$

where c is the sound speed, γ the specific heat ratio and Δu is the velocity jump reconstructed at the cell boundary. The term linear in Δu then gives, for a 3D simulation solving 1D Riemann problems in each direction:

$$\varepsilon_{\text{L}} = \sum -q_i^{\text{mono}} \frac{\partial u_i}{\partial x_i} = \sum \frac{1}{2}\rho c \Delta u_i \frac{\partial u_i}{\partial x_i} \tag{4}$$

The dissipation in the Lagrange phase does not vanish when $\nabla \cdot \mathbf{u} = 0$ and, when the Mach number is low, becomes greater than the diagonal terms in Equation (2).

In TURMOIL, dissipation does not increase as the Mach number is reduced since ε_{L} (Equation (1)) goes to zero for incompressible flow while ε_{R} (Equation (2)) is independent of the sound speed. This low Mach number behaviour in TURMOIL is better than many Godunov methods. However, work on improving the low Mach number behaviour of Godunov methods [8] may make them well suited for calculating compressible turbulent flow.

DOI: 10.1002/fld

4. 3D SIMULATIONS

3D simulations were carried out for a sector of the sphere centred at the equator, $\pi/2-\pi/8<\theta, \phi<\pi/2+\pi/8$. This reduces the computational resources needed and avoids the mesh singularity at $\theta=0$. The r-ordinates of the mesh are moved with the mean radial flow to reduce numerical diffusion, i.e. a semi-Lagrangian calculation is performed. Moreover, the angular zones are merged near the origin, $0<r_0<2.5$, and near the outer boundary, $11.3<r_0<12$, where r_0 denotes the initial radius. This overcomes the problem associated with the mesh singularity at the origin and also limits the 3D calculation to the region near the interface where mixing occurs. The number of zones used in the r, θ and ϕ directions is as follows: coarse: $220\times120\times120$; standard: $440\times240\times240$; fine: $880\times480\times480$. The latter ran for 160 h (wall clock time) using 288 processors of the AWE IBM SP.

Random amplitude perturbations are initially applied to the light fluid/dense fluid interface. The power spectrum used is $P(k)=Ck^{-2}$ if $k_{\min}<k<k_{\max}$, $P(k)=0$ otherwise. $k_{\min}=2\pi/(2.0)$ and $k_{\max}=2\pi/4\Delta s$, with Δs the radial mesh width at the interface. The constant C is chosen so that the s.d. of the perturbation is $\sigma=0.0005$, where $\sigma^2=\int_0^\infty P(k)\,\mathrm{d}k$.

Figure 3 shows sections from the standard mesh simulation. The shading represents the volume fraction of the denser fluid. The sector used in the computation has been repeated eight times to produce a full circle. Figure 4(a) shows the turbulent mixing zone limits *versus* time for the three simulations, i.e. the values of r at which the dense fluid volume fraction averaged over solid angle, $\langle f\rangle$, is equal to 0.01 and 0.99. Figure 4(b) shows distributions of the dense fluid volume fraction at the end of the simulations. The width of the mixing zone reduces slightly as the mesh is refined. However, the effect of mesh size is not very large and this suggests that the fine mesh calculation should give a good indication of the amount of mixing.

Figure 5(a) shows the distribution of resolved turbulence kinetic energy, k, at the end of the simulations. This is defined by $k\equiv\frac{1}{2}\langle\rho\{(u-\tilde{u})^2+v^2+w^2\}\rangle/\langle\rho\rangle$, where $\langle\cdot\rangle$ denotes the angular average and $\tilde{u}$ is the mass-weighted mean radial velocity. The kinetic energy dissipation in the Lagrange and remap phases, Equations (1) and (2), is shown in Figure 5(b). At $t=3$, when there are no significant shocks, dissipation in the Lagrangian phase is negligible as required. The results on the standard and fine meshes are similar for both characteristics.

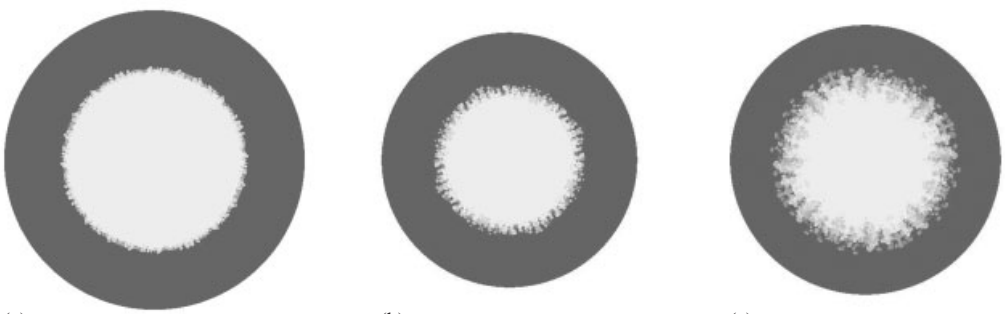

Figure 3. 2D sections through the 3D mesh for the spherical implosion, before, near and after maximum compression: (a) $t=2.0$; (b) $t=2.4$; and (c) $t=2.8$.

DOI: 10.1002/fld

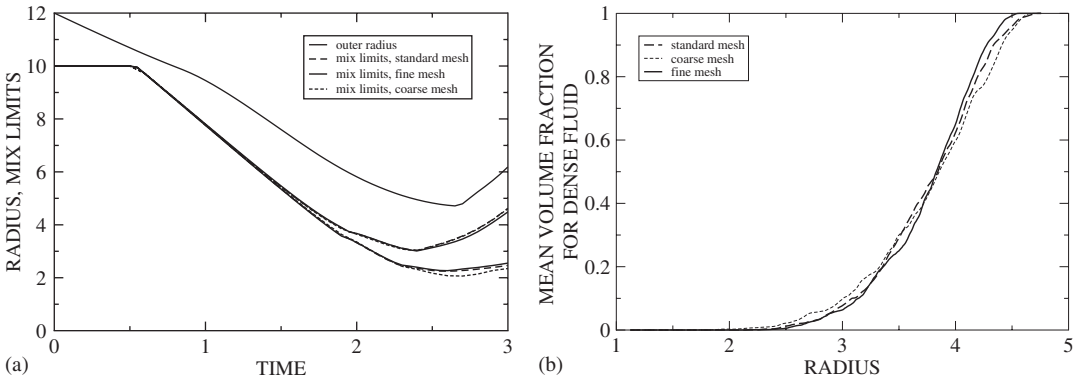

Figure 4. (a) Development of mixing zone width and (b) distributions of the dense fluid at $t = 3$.

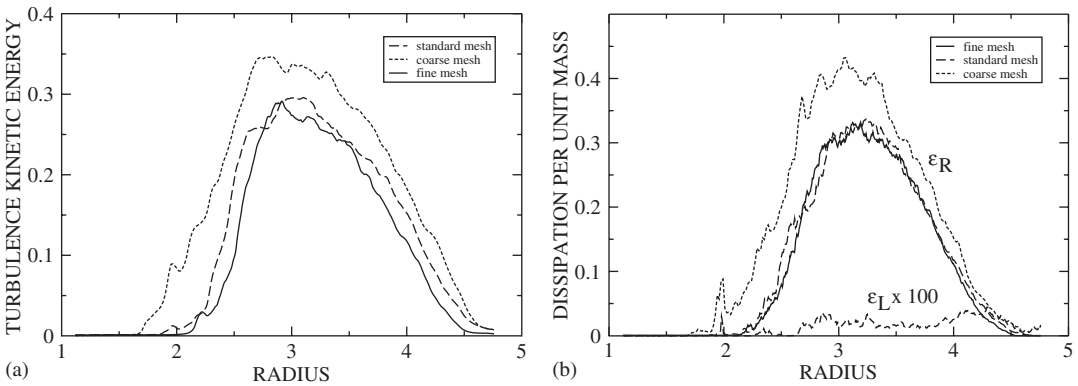

Figure 5. Flow characteristics at $t = 3$. (a) Resolved turbulence kinetic energy and (b) angle-averaged dissipation per unit mass. The dissipation in the remap phase, ε_R, is compared with ε_L, the dissipation in the Lagrange phase (due to shocks).

5. CONCLUSIONS

Accurate 3D numerical simulations have been performed for turbulent mixing in simple spherical implosions. Higher resolution simulations are planned in the near future using the AWE Cray XT3 (8000 processing elements) to confirm mesh convergence. The TURMOIL hydrocode used has good low Mach number behaviour, a key requirement for calculation of turbulent flow. The kinetic energy dissipation in the simulations has been accurately quantified. Our results suggest that the 'sub-grid' dissipation is close to being mesh converged. While detailed 3D simulation is impractical for many real problems, results of the type shown here are essential for calibrating and validating engineering models for use in real applications.

DOI: 10.1002/fld

REFERENCES

1. Youngs DL. Three-dimensional numerical simulation of turbulent mixing by Rayleigh–Taylor instability. *Physics of Fluids* 1991; **A3**:1312–1320.
2. Youngs DL. Numerical simulation of Rayleigh–Taylor and Richtmyer–Meshkov instabilities. *Laser and Particle Beams* 1994; **13**:725–750.
3. Guillard H, Murrone A. On the behaviour of upwind schemes in the low Mach number limit: II. Godunov type schemes. *Computers and Fluids* 2004; **33**:655–675.
4. Youngs DL. Time-dependent multi-material flow with large fluid distortion. In *Numerical Methods for Fluid Dynamics*, Morton KW, Baines MJ (eds). Academic Press: New York, 1982; 273–285.
5. DeBar R. A method in two-D Eulerian hydrodynamics. *Lawrence Livermore National Laboratory Report UCID-196831*, 1974.
6. Blondin JM, Chevalier RA, Frierson DM. Pulsar wind nebulae in evolved supernova remants. *Astrophysical Journal* 2001; **563**:806–815.
7. Benson DJ. Computational methods in Lagrangian and Eulerian hydrocodes. *Computer Methods in Applied Mechanics and Engineering* 1992; **99**:235–394.
8. Thornber B, Drikakis D. Numerical dissipation of upwind schemes in low Mach flow. *International Journal for Numerical Methods in Fluids* 2007, accepted. DOI: 10.1002/fld.1628.